Atmospheric
Measurement
Techniques

Supplement of

Characterization of a chemical modulation reactor (CMR) for the measurement of atmospheric concentrations of hydroxyl radicals with a laser-induced fluorescence instrument

Changmin Cho et al.

Correspondence to: Andreas Hofzumahaus (a.hofzumahaus@fz-juelich.de) and Anna Novelli (a.novelli@fz-juelich.de)

Table S1: Operational conditions of the CMR for the JULIAC campaigns

	Winter (I)	Spring (II)	Summer (III) and Autumn (IV)
Period	14 Jan. – 11 Feb.	9 Apr. – 6 May	4 Aug. – 2 Sep. 28 Oct. – 24 Nov.
Injector type	1/8" injectors	1/16" injectors	1/8" injectors
Carrier flow	500 sccm	200 - 300 sccm	500 sccm
Propane concentration	15 ppmv	15 - 25 ppmv	19 ppmv
Scavenging efficiency[a,b]	91%	> 85%	96%
Transmission[a,c]	64 %	75 %	64 %
Limit of detection[d]	0.7×10^6 cm^{-3}	0.8×10^6 cm^{-3}	0.6×10^6 cm^{-3}

a Determined in clean synthetic air ($k_{OH} = 0$).

b OH scavenging efficiency = $(1 - \alpha) \times 100\%$.

c OH transmission (β_{N2}) of the complete CMR.

d Signal-to-noise ratio = 1, averaging time: 45s.

* From 01.02.2019 to 11.02.2019 the CMR was not mounted.

Table S2: Summary of meteorological conditions and trace gas concentrations during JULIAC given as nighttime median values with 1σ standard deviations of ambient variabilities

	$OH / 10^6\ cm^{-3}$	NO / ppbv	O_3 / ppbv	H_2O / %[a]	k_{OH} / s^{-1}	k_{VOC}[b] / s^{-1}	T / °C
14 Jan. – 11 Feb.			22.8	0.6	6.3	2.5	2.4
			(±10.3)	(±0.2)	(±5.2)	(±2.0)	(±3.8)
9 Apr. – 6 May			40.1	0.7	5.8	3.2	10.0
			(±14.4)	(±0.2)	(±1.9)	(±1.3)	(±4.5)
4 Aug. – 2 Sep.	N/A[c]	N/A[c]	31.4	1.4	6.0	3.8	17.7
			(±14.5)	(±0.3)	(±2.8)	(±2.2)	(±3.8)
28 Oct. – 24 Nov.			15.0	0.7	6.5	2.4	4.6
			(±9.3)	(±0.2)	(±3.8)	(±1.5)	(±4.4)

a Volume mixing ratio

b OH reactivity of non-methane VOCs, calculated as the difference between measured total k_{OH} and the sum of calculated reactivities of CH_4, CO, O_3, NO, and NO_2.

c Below the limit of the detection.
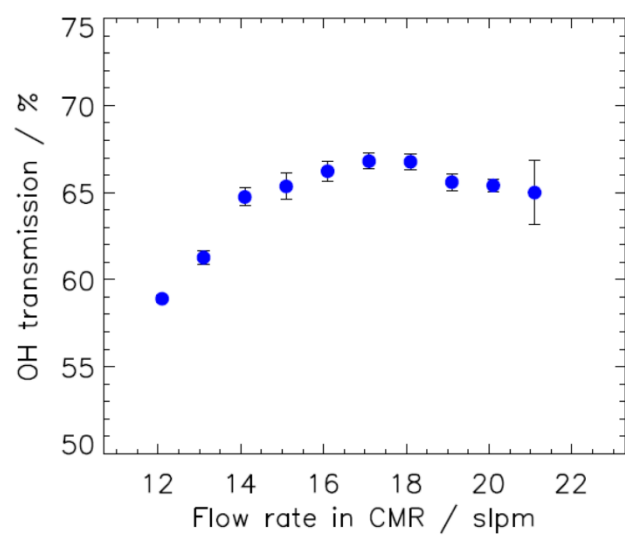
Figure S1: OH radical transmission measured while varying the flow rate in the CMR.
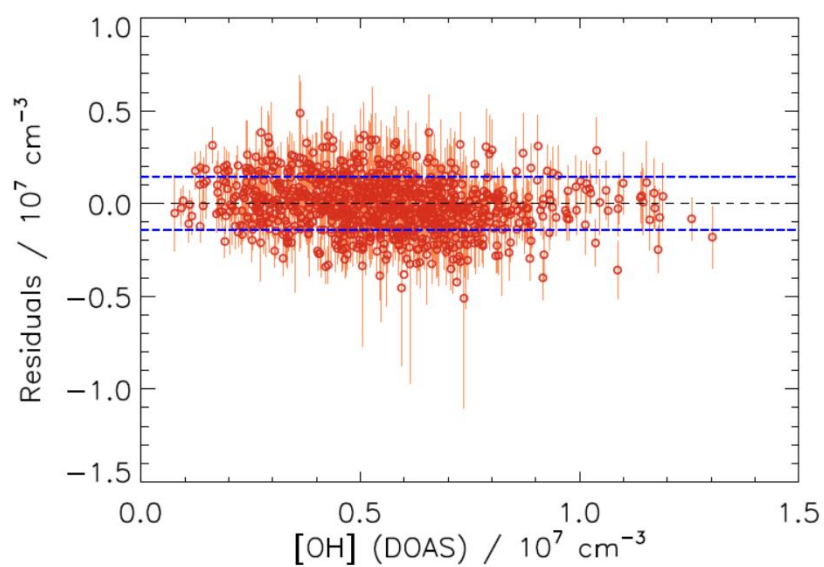
Figure S2: Residuals of the OH concentrations measured by FZJ-LIF-CMR , obtained from the difference between the measured OH concentrations and the linear fit shown in Figure 12 plotted vs the OH concentrations measured by DOAS. Vertical bars denote the combined 1σ precision of the measured data points from the both instruments. Blue dashed lines represent the value of the standard deviation of the residuals.
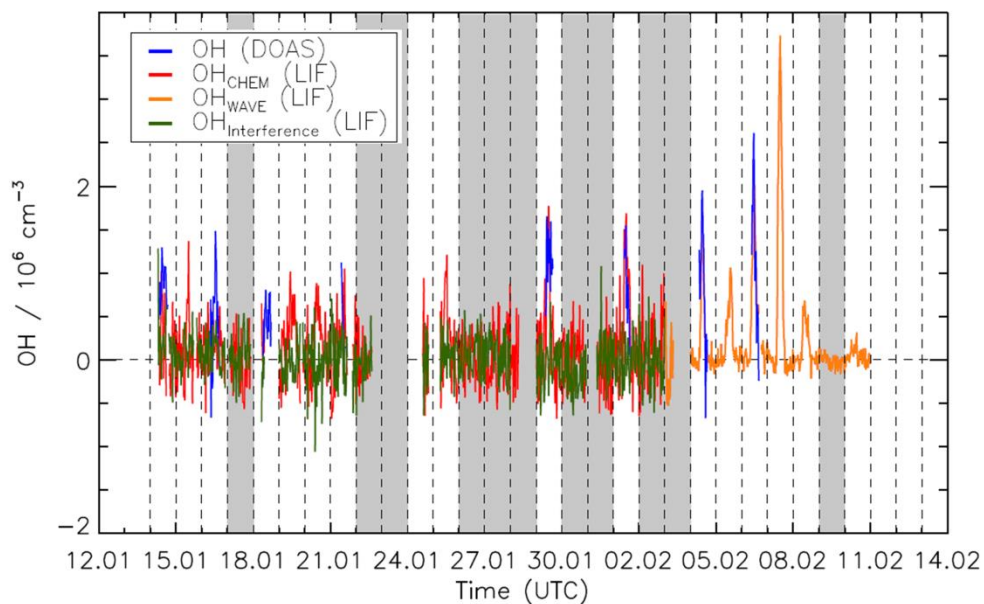
Figure S3: Measured OH concentration and OH interference by LIF with the CMR and DOAS during winter (I) intensive. All data sets are 30 min average. Dashed lines denote midnights. Grey boxes indicate when the roof was closed.
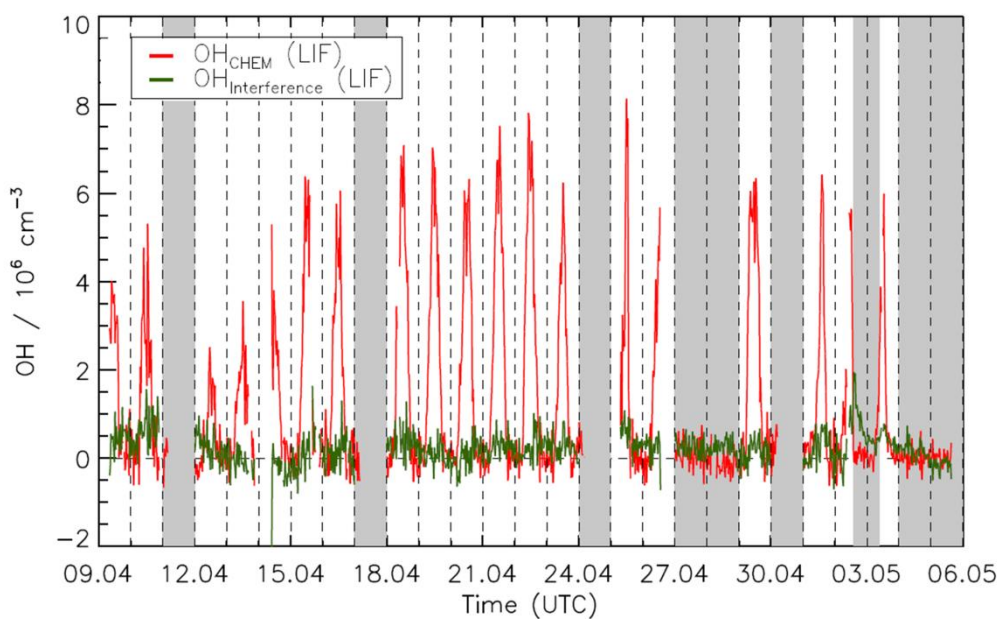
Figure S4: Measured OH concentration and OH interference by LIF with the CMR during spring (II) intensive. All data sets are 30 min average. Dashed lines denote midnights. Grey boxes indicate when the roof was closed.
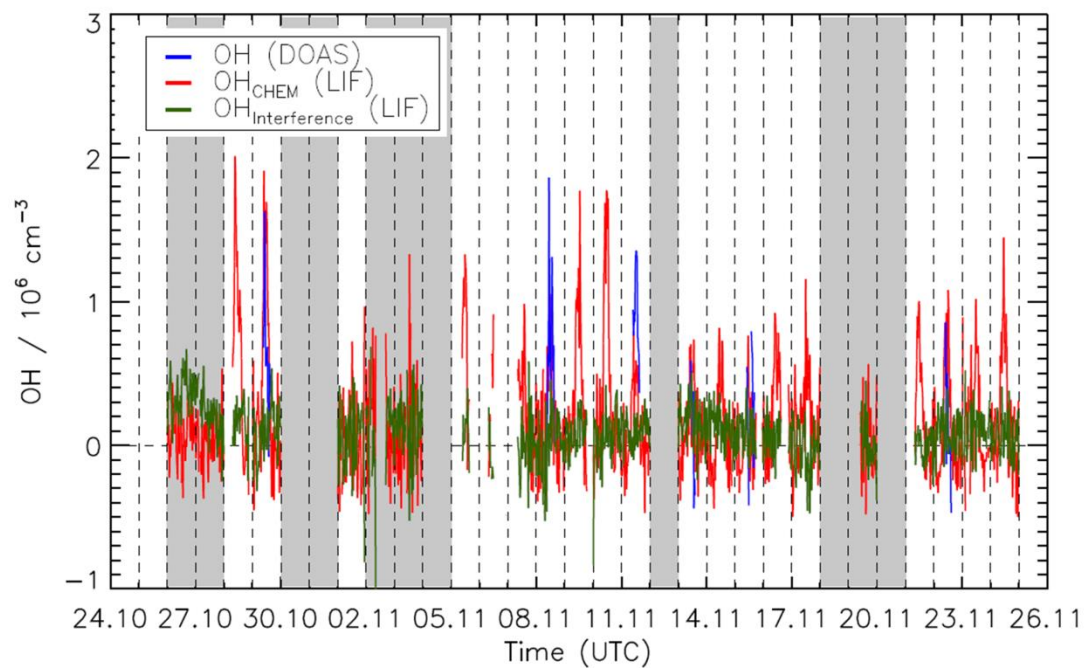
Figure S5: Measured OH concentration and OH interference by LIF with the CMR and DOAS during autumn (IV) intensive. All data sets are 30 min average. Dashed lines denote midnights. Grey boxes indicate when the roof was closed.